Communication

Israel Journal of Chemistry
www.ijc.wiley-vch.de

doi.org/10.1002/ijch.202300017

Metal-Organic Frameworks with Rod Yttrium Secondary Building Units

Zhiling Zheng,[a, b, c] Zichao Rong,[a, b, c] Oscar Iu-Fan Chen,[a, b, c] and Omar M. Yaghi*[a, b, c]

Dedicated to Professor Helmut Schwarz on the occasion of his 80th birthday.

Abstract: We report a new hydroxamate-based yttrium MOF, named MOF-419 [Y(HCOO)(BDH)], with rod-SBUs. The compound was synthesized employing chelating construction of benzene-1,4-hydroxamate (BDH^{2-}) linkers, and the use of formic acid as the modulator was found to be crucial for the formation of rod-shaped SBUs. MOF-419 shows permanent porosity and has a BET surface area of 1130 m^2/g. Its hydrophobic pore environment and gas sorption properties were demonstrated through the combination of single crystal X-ray diffraction and nitrogen, carbon dioxide, and water sorption experiments. We envision that these results will aid the study and understanding of rod MOFs with chelating linkages.

Keywords: metal-organic frameworks · crystal structures · hydroxamate · yttrium · porosity

Metal-organic frameworks (MOFs) consisting of rod-like metal-containing secondary building units (SBUs) are known to exhibit favorable sorption properties.[1] They also have exceptional chemical stability, particularly towards water, which is attributed to the steric shielding of the metal ions by the linkages.[2] In addition, the channels within the framework enclosed by the rod packings are highly open, allowing for the free and fast movement of guest molecules.[3] Due to these attractive features, rod MOFs are generally considered to be more desirable candidates compared to MOFs constructed from other SBUs (i.e., discrete metal clusters), making them promising and durable materials for applications such as catalysis,[4] gas separation,[5] sensing,[6] pollutant removal,[7] and water harvesting.[2a,8] One well-known example of a rod MOF is the state-of-art water-harvesting material MOF-303 [Al(OH)(PZDC), where $PZDC^{2-}$ is 1*H*-pyrazole-3,5-dicarboxylate], which exhibits impressive hydrolytic stability and fast kinetics during cycling.[1c,9] While it is important to discover and study the novel rod MOFs for various applications, synthesizing these materials remains challenging due to the lack of a general guiding principle and the tendency for linkers to inhibit the formation of chains through complex polydentate chelating mechanisms.[10] Additionally, the majority of linker functionalities in rod-like SBUs are limited to carboxylates, with some less common examples including phosphonates, azolates, and mixed functionalities.[1a] As a result, the variety of rod MOFs remains to be expanded through the development of new types of linkage.

It has been recently discovered that linkers containing hydroxamate groups can be used to construct MOFs.[11] Known for their strong bonding with metals, these chelating linkers are expected to enhance the stability and diversity of extended structures, as they are sterically unencumbered with a linking pattern similar to commonly used carboxylate linkers, but have different coordination bonding strength and geometry. Furthermore, the presence of an –NH group on the hydroxamate linker may increase the hydrophilicity of the pore environment and provide an additional adsorption site for guest molecules. However, this field in reticular chemistry is still underdeveloped, and only a few hydroxamate MOFs with discrete metal clustered-based SBUs have been reported.[11a–d] To date, rod MOFs remain largely unexplored because of difficulties in obtaining crystals and making frameworks with permanent porosity.[12] By using the benzene-1,4-hydroxamic acid (H_2BDH) linker (Scheme 1), which is structurally similar to the abundant benzene-1,4-dicarboxylate (H_2BDC) linker

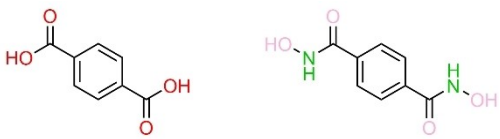

Scheme 1. Structure of carboxylate-based H_2BDC linker (left) and hydroxamate-based H_2BDH linker (right).

[a] *Z. Zheng, Z. Rong, O. Iu-Fan Chen, O. M. Yaghi*
Department of Chemistry, University of California Berkeley, California, 94720, U.S.A.
E-mail: yaghi@berkeley.edu
[b] *Z. Zheng, Z. Rong, O. Iu-Fan Chen, O. M. Yaghi*
Kavli Energy NanoSciences Institute Berkeley, California, 94720, U.S.A.
[c] *Z. Zheng, Z. Rong, O. Iu-Fan Chen, O. M. Yaghi*
Bakar Institute of Digital Materials for the Planet, Division of Computing, Data Science, and Society, University of California Berkeley, California, 94720, U.S.A.

Supporting information for this article is available on the WWW under https://doi.org/10.1002/ijch.202300017

commonly used in the synthesis of rod MOFs,[1a] in combination with a suitable structural-directing modulator (HCOOH), we aim to overcome these challenges and successfully synthesize hydroxamate-based rod MOFs.

Herein, we report the first Y-hydroxamate framework, MOF-419 [Y(HCOO)(BDH)], and its structural and sorption properties. We synthesized this rod-MOF through a solvothermal reaction of $Y(NO_3)_3 \cdot 6H_2O$ and H_2BDH in N, N-dimethylformamide (DMF) with formic acid as the modulator, resulting in the formation of light-pink needle-shaped crystals after 90 min at 100 °C (Figure S1, Supporting information). Alternatively, MOF-419 crystals can be synthesized using a green synthesis procedure with H_2O as solvent under similar synthesis condition (Section S2, Supporting information).

Single crystal X-ray diffraction studies showed that MOF-419 crystals have $I4_122$ space group with unit cell parameters of $a = 17.2055(1)$ Å and $c = 15.7079(1)$ Å. Its rod-like SBU consists of edge-sharing YO_8 polyhedra, each in the form of a trigonal dodecahedron, connected by hydroxamates and carboxylates from terminal formates (Figure 1a and Section S3, Supporting information). The Y centers are bound to four hydroxamate groups from four linkers, where two hydroxamates are bidentate and the remaining two are monodentate. The Y coordination sphere is completed with oxygen from two formates bridging two Y^{3+} ions (Figure 1b). The BDH linkers are bonded to four polyhedrons from two chains (Figure 1c, Figure S2, and Figure S3, Supporting information). This leads to a 3D framework supporting square-shaped 1D channels of around 9 Å (Figure 1d). In terms of topology, the underlying net of MOF-419 is described as a **snp** rod net in which the points of extension are defined by the carbon atoms on the hydroxamate units.[1a,13]

It should be acknowledged that current strategies to obtain rod-MOFs remain limited. In addition to a previously demonstrated approach utilizing vicinal dicarboxylates as the linker,[14] the successful synthesis of rod MOF-419 represents a new strategy involving a hydroxamate linker and modulator. As depicted in Figure 1b, an important observation is the distinctive binding behavior of the organic linker. While the 5-member ring exhibits favorable chelation, the 4-member ring does not, resulting in carboxylates acting as bridging units rather than chelating units. Intriguingly, the hydroxamate acts as both chelating and bridging units. We attribute the formation of rod-SBUs in this case to the precise mixture of only bridging (formate) units and chelating-bridging (hydroxamate) units. It is worth noting that without the use of formate, no MOF product was obtained under identical conditions.

With the crystal structure elucidated by SXRD, the phase purity of prepared MOF-419 was confirmed by comparing the experimental powder X-ray diffraction (PXRD) pattern with the simulated pattern based on SXRD data (Figure 2a). We observed that after activation, both MOF-419 samples prepared via hydrothermal synthesis and DMF-based synthesis displayed high crystallinity in their PXRD patterns, in addition to having a good agreement with the simulations. This indicates that the same pure phase of MOF-419 was obtained using different solvents (Figure S4, Supporting information). We used SEM primarily to examine if the activated MOF-419 sample has homogeneous morphology and particle sizes within the same batch (Figure S12 and Figure S13, Supporting Information). The result showed that only needle-shaped crystallites were found with little variation in particle size.

To probe the composition of MOF-419, the activated samples were subject to NMR spectroscopy and elemental analysis (EA). The results showed that no impurity was presented and that DMF or other solvents were removed from the activated MOF (Table S1 and Figure S7, Supporting information). Remarkably, the hydroxamate linker BDH^{2-} and formate ligand $HCOO^-$ were found to present in a 1 : 1 ratio, which is in agreement with the chemical formula Y-(BDH)(HCOO) derived from the single-crystal structure. These findings indicate that the use of formic acid as the modulator is the key to obtaining this rod MOF, whose SBU was otherwise structurally unachievable without the formate ligand. This approach may be a useful strategy for constructing other hydroxamate-based MOFs with rod-like SBUs.

To investigate the chemical stability of MOF-419, the crystals were placed in a wide range of acidic and basic aqueous solutions at room temperature for 7 days. The PXRD data showed that the crystallinity did not change within the pH range of 3–13, suggesting the retention of integrity of the crystal structure under these conditions (Figure 2b). This is likely due to the chelating nature of the hydroxamate linker and the steric shielding of metal ions under rod SBUs. In addition, the thermal stability of MOF-419 was investigated by thermogravimetric analysis (Figure S8 and Figure S9, Supporting information). The results show that the overall performance of MOF-419 in terms of chemical and thermal stability is similar to other reported hydroxamate-based MOFs.[11]

The porosity of MOF-419 was probed using nitrogen sorption analysis measured at 77 K (Figure 2c). Notably, it exhibited a typical type IV isotherm with a pronounced adsorption-desorption hysteresis loop between $P/P_0 = 0.2$ and 0.7, likely due to the flexibility in the bonding between the hydroxamate group and the rod-SBU (Figure S2, Supporting information). The surface area was calculated to be 1130 m^2/g from the Brunauer-Emmett-Teller (BET) model by fitting the selected adsorption points that met the consistency criteria for the BET theory (Figure S10, Supporting information). The pore size distribution of MOF-419 was derived by fitting the nonlinear density functional theory (NLDFT) model to the collected nitrogen isotherm and the total pore volume was determined to be 0.36 cm^3/g (Figure S11, Supporting information). A consistent homogeneous pore diameter of 1.1 nm from the analysis was found, which is in agreement with the 0.9 nm diameter determined from the crystal structure. The slight deviation between the two methods could be due to the presence of solvent molecules or the non-rigid nature of MOF-419.

The adsorption properties of MOF-419 were further investigated through other gases (Figure 1c). Its CO_2 sorption

Israel Journal of Chemistry

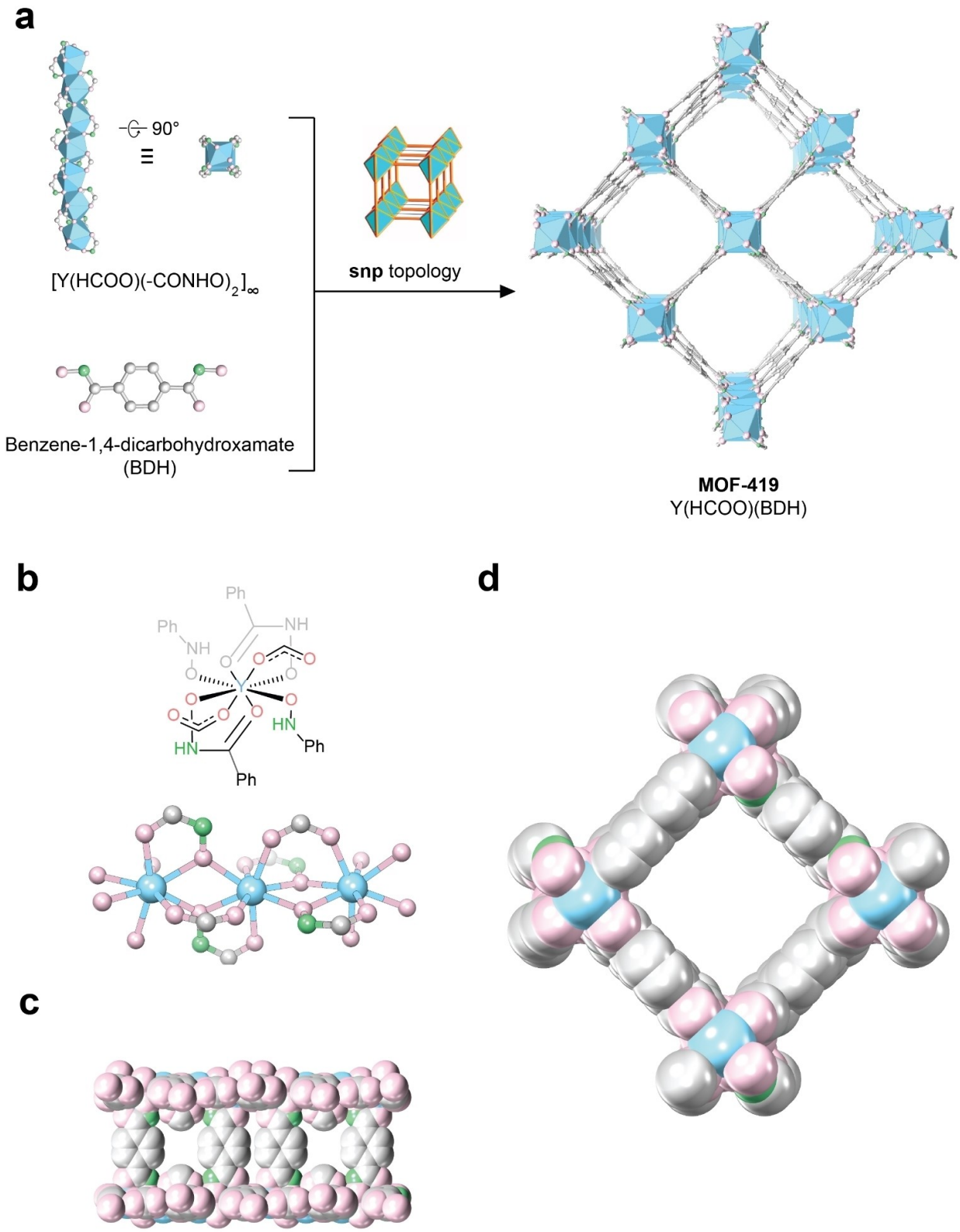

Figure 1. (a) Single crystal X-ray structure of MOF-419 constructed from the infinite rod-like secondary building units and chelating organic liniker H_2BDH with an underlying **snp** topology. (b) Coordination environment of secondary buiilding units in MOF-419. Each yitrrium atom is eight-coordinated and bonded to oxygen atoms from the hydroxamate groups and formate ligands. (c) The secondary building units are bridged by H_2BDH linkers in the middle to form a 3D structure supporting a 1D pore system. (d) The channel viewed along the *c* axis. Color code: Y, blue; O, pink; N, green; C, gray. Hydrogen atoms are omitted for clarity.

Israel Journal of Chemistry

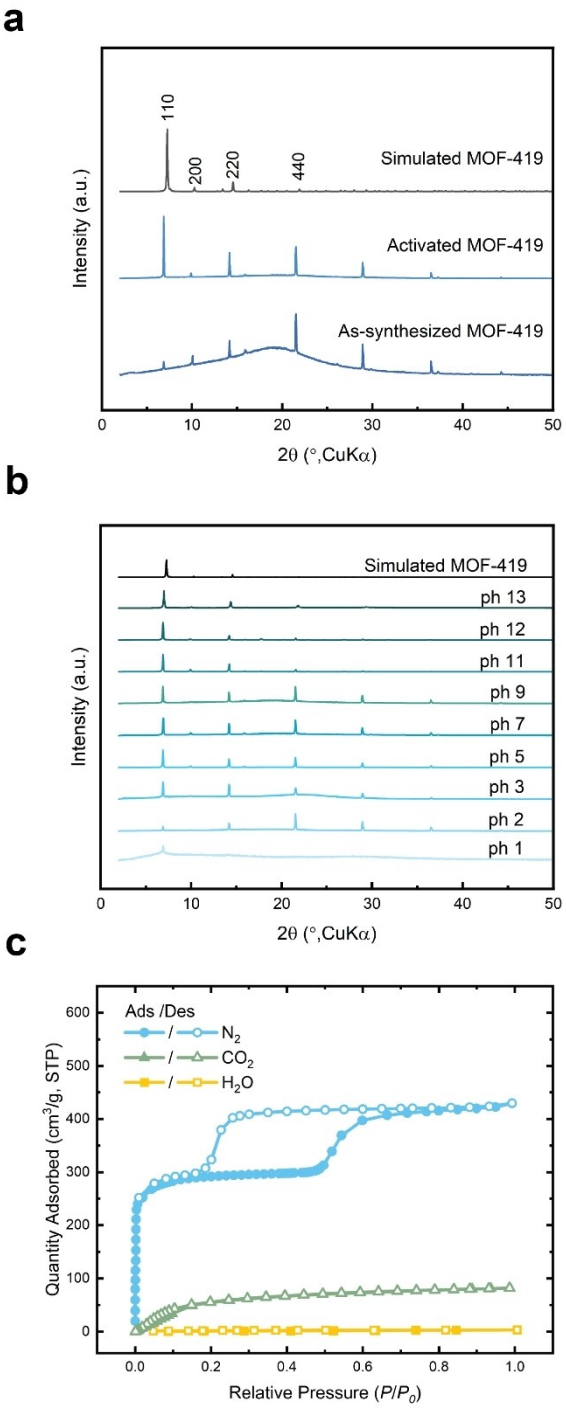

Figure 2. (a) PXRD patterns of as-synthesized and fully washed MOF-419. The simulated patterns at the bottom were generated using single crystal structure of MOF-419. (b) PXRD patterns of MOF-419 after exposure to aqueous solutions of different pH for 7 days. (c) Adsorption-desorption isotherms of nitrogen, carbon dioxide, and water vapor on MOF-419 at a measurement temperature of 77 K for nitrogen and 298 K for carbon dioxide and water vapor.

measured at 298 K showed a reversible type-I isotherm and a modest gravimetric uptake of 3.65 mmol·g^{-1} of CO_2 at 1 atm (16.1 wt %). Similarly, its water isotherm at 298 K revealed a maximum water uptake of 5.0 wt %, which is consistent with the observation that the sample showed no significant weight gain when stored under ambient conditions. This can be interpreted by the hydrophobic and non-polar pore environment of MOF-419. While the pore size of this MOF is approximately 1.1 nm as determined from crystallographic data, the 1D pore system within the channels lacks primary adsorption sites that have a strong affinity for carbon dioxide and water molecules.[15] Specifically, in terms of water sorption, compared to previously reported state-of-art water harvesting rod MOFs,[2a,8a,b,9b,16] MOF-419 has hydroxamate groups (–CONHOH) and formate ligands (HCOO) in place of carboxylic groups (–COOH) and bridging hydroxy groups (–OH), respectively, which are considered binding sites for water molecules. As suggested by the crystal structure of MOF-419 (Figure 1d), potential primary adsorption sites such as –NH and –COO are not easily accessible by those water molecules passing through the channel, as their geometry relation is unlike the one of hydrophilic atoms and hydroxyl groups in water harvesting MOFs such as MOF-303. Additionally, the more hydrophobic phenyl rings dominate the backbone of the framework, which leads to a low ratio between the accessible hydrophilic sites and hydrophobic sites in MOF-419. Consequently, they together discourage the residence of the very first water molecules in the pore to form small water aggregated seeds and making hydrogen bonds. As for the carbon dioxide molecules, despite MOF-419's high surface area and large pore opening, both the metal sites and polar atoms in this MOF are less accessible, resulting in weaker dipole-dipole interactions between CO_2 and MOF backbone and hindering the uptake of CO_2.

Acknowledgements

We thank the financial support from Defense Advanced Research Projects Agency (DARPA) under contract HR0011-21-C-0020. Any opinions, findings, conclusions, or recommendations expressed in this material are those of the author(s) and do not necessarily reflect the views of DARPA. Z.Z. thanks Drs. Xiaokun Pei and Xing Han from the Yaghi Research Group for their helpful discussions. We thank Dr. Nikita Hanikel, Mr. Kaiyu Wang, and Mr. Ephraim Neumann from the Yaghi Research Group for water vapor and carbon dioxide sorption measurements, and SEM image measurements, respectively. Z.Z. thanks for the financial support through a Kavli ENSI Graduate Student Fellowship. O.I.-F.C. acknowledges financial support from the Taiwan Ministry of Education. We acknowledge the College of Chemistry Nuclear Magnetic Resonance Facility and Small Molecule X-ray Crystallography Facility for resource instruments and staff assistance from Dr. Nicholas Settineri.

Israel Journal of Chemistry

Data Availability Statement

The data that support the findings of this study are available on request from the corresponding author. The data are not publicly available due to privacy or ethical restrictions.

References

[1] a) A. Schoedel, M. Li, D. Li, M. O'Keeffe, O. M. Yaghi, *Chem. Rev.* **2016**, *116*, 12466; b) M. J. Kalmutzki, N. Hanikel, O. M. Yaghi, *Sci. Adv.* **2018**, *4*, eaat9180; c) F. Fathieh, M. J. Kalmutzki, E. A. Kapustin, P. J. Waller, J. Yang, O. M. Yaghi, *Sci. Adv.* **2018**, *4*, eaat3198.

[2] a) N. Hanikel, X. Pei, S. Chheda, H. Lyu, W. Jeong, J. Sauer, L. Gagliardi, O. M. Yaghi, *Science* **2021**, *374*, 454; b) N. Hanikel, M. S. Prévot, O. M. Yaghi, *Nat. Nanotechnol.* **2020**, *15*, 348.

[3] W. Xu, O. M. Yaghi, *ACS Cent. Sci.* **2020**, *6*, 1348.

[4] a) H. Jiang, X. Zhao, W. Zhang, Y. Liu, H. Li, Y. Cui, *Angew. Chem.* **2023**, *135*, e202214748; b) S. Zhao, C. Tan, C.-T. He, P. An, F. Xie, S. Jiang, Y. Zhu, K.-H. Wu, B. Zhang, H. Li, *Nat. Energy* **2020**, *5*, 881.

[5] a) H. Wang, Z. Shi, J. Yang, T. Sun, B. Rungtaweevoranit, H. Lyu, Y. B. Zhang, O. M. Yaghi, *Angew. Chem. Int. Ed.* **2021**, *60*, 3417; b) H. Furukawa, K. E. Cordova, M. O'Keeffe, O. M. Yaghi, *Science* **2013**, *341*, 1230444.

[6] A. Douvali, A. C. Tsipis, S. V. Eliseeva, S. Petoud, G. S. Papaefstathiou, C. D. Malliakas, I. Papadas, G. S. Armatas, I. Margiolaki, M. G. Kanatzidis, *Angew. Chem.* **2015**, *127*, 1671.

[7] a) T. G. Glover, G. W. Peterson, B. J. Schindler, D. Britt, O. Yaghi, *Chem. Eng. Sci.* **2011**, *66*, 163; b) W. Wang, F. Yang, Y. Yang, Y.-Y. Wang, B. Liu, *J. Agric. Food Chem.* **2022**; c) X. Han, S. Yang, M. Schröder, *Nat. Chem. Rev.* **2019**, *3*, 108.

[8] a) D. Lenzen, J. Zhao, S.-J. Ernst, M. Wahiduzzaman, A. Ken Inge, D. Fröhlich, H. Xu, H.-J. Bart, C. Janiak, S. Henninger, *Nat. Commun.* **2019**, *10*, 1; b) K. H. Cho, D. D. Borges, U. Lee, J. S. Lee, J. W. Yoon, S. J. Cho, J. Park, W. Lombardo, D. Moon, A. Sapienza, *Nat. Commun.* **2020**, *11*, 1; c) M. Silva, A. Ribeiro, C. Silva, I. Nogueira, K.-H. Cho, U. Lee, J. Faria, J. Loureiro, J.-S. Chang, A. Rodrigues, *Adsorption* **2021**, *27*, 213; d) Z. Zheng, A. H. Alawadhi, O. M. Yaghi, *Mol. Front. J.* **2023**, 1.

[9] a) N. Hanikel, M. S. Prévot, F. Fathieh, E. A. Kapustin, H. Lyu, H. Wang, N. J. Diercks, T. G. Glover, O. M. Yaghi, *ACS Cent. Sci.* **2019**, *5*, 1699; b) Z. Zheng, N. Hanikel, H. Lyu, O. M. Yaghi, *J. Am. Chem. Soc.* **2022**, *144*, 22669.

[10] S. Won, S. Jeong, D. Kim, J. Seong, J. Lim, D. Moon, S. B. Baek, M. S. Lah, *Chem. Mater.* **2021**, *34*, 273.

[11] a) C. F. Pereira, A. J. Howarth, N. A. Vermeulen, F. A. A. Paz, J. P. Tomé, J. T. Hupp, O. K. Farha, *Mater. Chem. Front.* **2017**, *1*, 1194; b) N. M. Padial, J. Castells-Gil, N. Almora-Barrios, M. Romero-Angel, I. Da Silva, M. Barawi, A. Garcia-Sanchez, V. C. A. de la Peña O'Shea, C. Marti-Gastaldo, *J. Am. Chem. Soc.* **2019**, *141*, 13124; c) Q. Lai, Z.-Q. Chu, X. Xiao, D. Dai, T. Song, T.-Y. Luo, W. Tang, X. Feng, Z. Zhang, T. Li, *Chem. Commun.* **2022**, *58*, 3601; d) J. A. Chiong, J. Zhu, J. B. Bailey, M. Kalaj, R. H. Subramanian, W. Xu, S. M. Cohen, F. A. Tezcan, *J. Am. Chem. Soc.* **2020**, *142*, 6907; e) J. Zhu, L. Samperisi, M. Kalaj, J. A. Chiong, J. B. Bailey, Z. Zhang, C.-J. Yu, R. E. Sikma, X. Zou, S. M. Cohen, *Dalton Trans.* **2022**, *51*, 1927.

[12] a) Y. Yan, N.-N. Zhang, D. Fuhrmann, S. Merker, H. Krautscheid, *Dalton Trans.* **2022**, *51*, 15946; b) X. Feng, W. Li, L. Yang, T. Song, Z. Xia, Q. Lai, X. Zhou, H. Xiao, C. Liu, *Chem. Commun.* **2022**, *58*, 13503.

[13] M. O'Keeffe, O. M. Yaghi, *Chem. Rev.* **2012**, *112*, 675.

[14] F. M. A. Noa, M. Abrahamsson, E. Ahlberg, O. Cheung, C. R. Göb, C. J. McKenzie, L. Öhrström, *Chem* **2021**, *7*, 2491.

[15] a) H. Furukawa, F. Gandara, Y.-B. Zhang, J. Jiang, W. L. Queen, M. R. Hudson, O. M. Yaghi, *J. Am. Chem. Soc.* **2014**, *136*, 4369; b) C.-H. Liu, H. L. Nguyen, O. M. Yaghi, *ACM* **2020**, *1*, 18; c) A. Cadiau, J. S. Lee, D. Damasceno Borges, P. Fabry, T. Devic, M. T. Wharmby, C. Martineau, D. Foucher, F. Taulelle, C. H. Jun, *Adv. Mater.* **2015**, *27*, 4775.

[16] a) Z. Zheng, H. L. Nguyen, N. Hanikel, K. K.-Y. Li, Z. Zhou, T. Ma, O. M. Yaghi, *Nat. Protoc.* **2023**, *18*, 136; b) D. Lenzen, P. Bendix, H. Reinsch, D. Fröhlich, H. Kummer, M. Möllers, P. P. Hügenell, R. Gläser, S. Henninger, N. Stock, *Adv. Mater.* **2018**, *30*, 1705869; c) N. Hanikel, D. Kurandina, S. Chheda, Z. Zheng, Z. Rong, S. E. Neumann, J. Sauer, J. I. Siepmann, L. Gagliardi, O. M. Yaghi, *ACS Cent. Sci.* **2023**.

Manuscript received: January 31, 2023
Revised manuscript received: March 8, 2023
Version of record online: March 29, 2023